Carbohydrate Polymer Technologies and Applications 11 (2025) 100996

Contents lists available at ScienceDirect

Carbohydrate Polymer Technologies and Applications

journal homepage: www.sciencedirect.com/journal/carbohydrate-polymer-technologies-and-applications

Synthesis, characterization and structural elucidation of a new sodium β-cyclodextrin-based metal-organic framework and the sodium chloride β-cyclodextrin inclusion complex

Amine Ez-zoubi [a], Saskia Merz-Chulbi [b], Nicolás Moliner [b], Rafael Ruiz-García [b], Abdellah Farah [a], Salah-Eddine Stiriba [b,*]

[a] Laboratory of Applied Organic Chemistry, Faculty of Sciences and Techniques, Sidi Mohamed Ben Abdellah University, Route d'Imouzzer, Fez, Morocco
[b] Instituto de Ciencia Molecular (ICMol), Universidad de Valencia, 46980 Paterna, Valencia, Spain

ARTICLE INFO

Keywords:
β-cyclodextrin
MOFs
Inclusion complexes
Host-guest interactions
Sodium

ABSTRACT

In this work, a new sodium-based metal-organic framework with the oligosaccharide β-cyclodextrin (**Na-βCD**) was synthesized and characterized using a set of experimental techniques, and the sodium chloride β-cyclodextrin inclusion complex (**NaCl-β-CD**) was also prepared and its crystal structure elucidated. **Na-β-CD** was achieved *via* tetrahydrofuran vapor diffusion in a dimethylformamide solution of β-CD using for the first time sodium hydride (NaH) as a base in 1:1 molar ratio of NaH/β-CD. Subsequently, **NaCl-β-CD** was obtained by recrystallization of the prepared **Na-β-CD** in an aqueous solution of NaCl (1:1 molar ratio). SEM-EDX analysis showed the characteristic Na peaks for both compounds (1:1 Na/β-CD molar ratio) together with the Cl peaks only for **NaCl-βCD** (1:1 Cl/β-CD molar ratio), while ^{1}H NMR and FTIR spectra indicated that both compounds retain the β-CD skeleton, with minor modifications attributed to β-CD deprotonation in **Na-β-CD** and sodium coordination in both compounds. In fact, **NaCl-β-CD** exhibits a $P2_1$ space group and its crystal structure reveals the formation of a sodium(I)-β-cyclodextrin double chain coordination polymer, whereas the hydrated Cl^- ions are encapsulated within the bowl-like internal cavities of β-CD through hydrogen bonding interactions forming a host-guest $(H_2O)_nCl\subset$β-CD inclusion complex. Consequently, this result demonstrates the ability of **Na-βCD** to incorporate chloride ions from aqueous solutions, and it paves the way for further research to extend the scope of β-CD-MOF-based materials.

1. Introduction

Cyclodextrins (CDs) are a type of cyclic oligosaccharides valued for their low cost, non-toxicity, biodegradability, and versatility to form inclusion complexes (ICs) both in solution and solid state (Wang et al., 2023; Cova et al., 2018). Such properties allow their use in a wide range of applications, including drug delivery (Singh & Mahar, 2024), catalysis (Payamifar & Marjani, 2024; Payamifar et al., 2024), and water remediation of inorganic and organic pollutants (Urooj et al., 2024). CDs are classified based on the number of glucose units in their structure; beta-cyclodextrin (β-CD) consisting of seven glucose units, is notable for its internal hydrophobic cavity, which is well-suited for encapsulating pharmaceutical compounds. It also offers a higher loading capacity and a more practical cost compared to other native cyclodextrins, including alpha-cyclodextrin (α-CD, six glucose units) and gamma-cyclodextrin (γ-CD, eight glucose units) (Ez-zoubi et al., 2025).

Of particular interest is the ability of β-CD to encapsulate guest molecules, either entirely or partially, within its hydrophobic inner cavity, resulting in the formation of host-guest ICs (Douhal, 2004). Their unique cage-like (truncated cone) structures render them highly desirable for the formation of ICs where the internal non-polar host cavity could interact *via* various non-covalent interactions, such as hydrogen bonding, van der Waals forces, and apolar-apolar affinities, with the guest ion or molecule (Chart 1) (Crini et al., 2018; Crini, 2014; Kfoury & Fourmentin, 2023; Ez-zoubi et al., 2024). Single-crystal X-ray diffraction studies of discrete β-CD ICs have been conducted, providing detailed insights into the role of these weak interactions in facilitating and stabilizing the host-guest assemblies (Liu & Liu, 2022; Prochowicz et al., 2017).

The structures of ICs established between β-CD and diverse guests

* Corresponding author.
E-mail address: stiriba@uv.es (S.-E. Stiriba).

https://doi.org/10.1016/j.carpta.2025.100996

Available online 4 September 2025

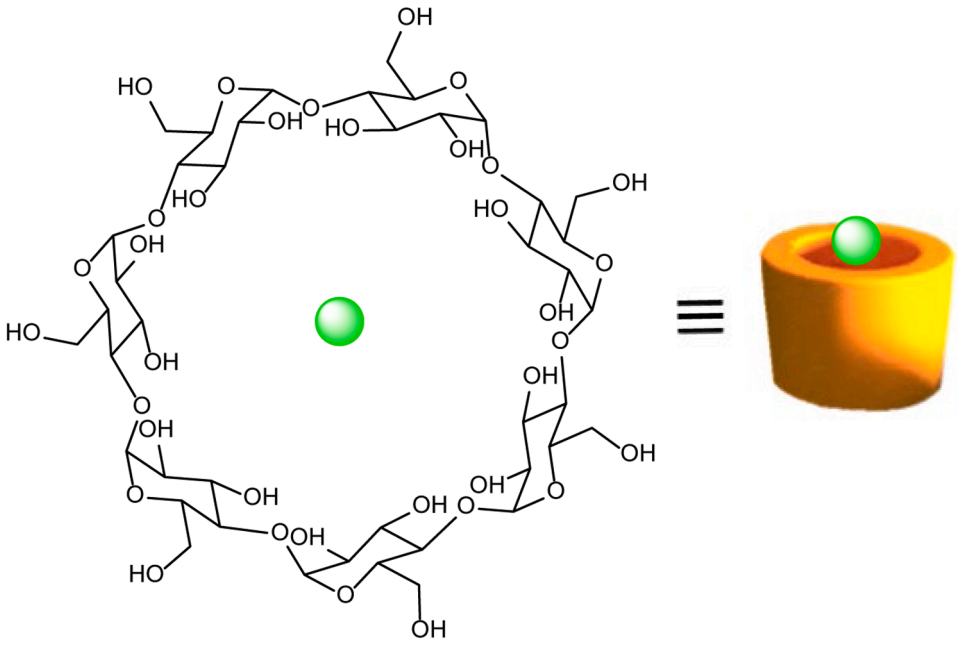

Chart 1. Host-guest inclusion complex resulting from β-cyclodextrin as host.

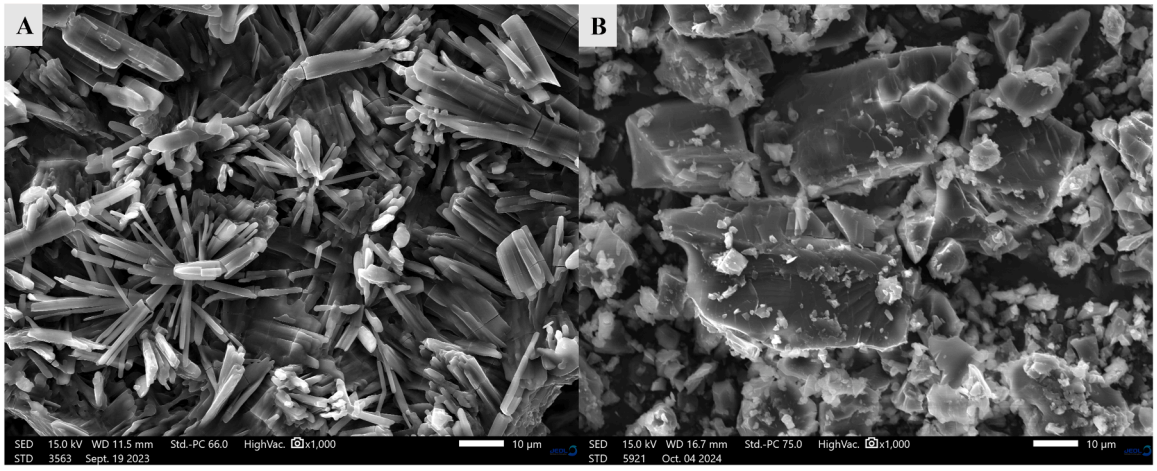

Fig. 1. Micrographs of Na-β-CD (A) and NaCl-β-CD (B).

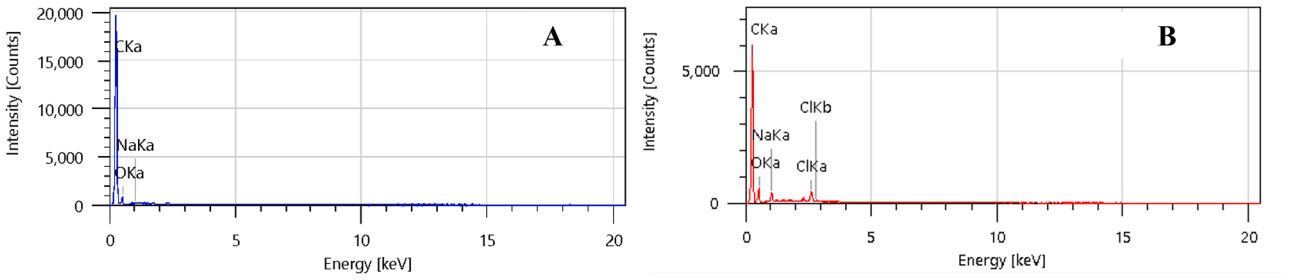

Fig. 2. EDX spectra of Na-β-CD (A) and NaCl-βCD (B).

have received considerable attention in health and pharmaceutical applications. In line with this, the crystal structure of β-CD ICs with natural bioactive molecules have been identified including cholesterol (Christoforides et al., 2018), catechin and epicatechin (Aree & Jongrungruangchok, 2016), and coffee chlorogenic acid (Aree, 2019). Indeed, multiple drugs have been identified by using crystallographic analysis, including aspirin (Nishioka et al., 1984), atenolol (Borodi et al., 2008), flurbiprofen (Betlejewska-Kielak et al., 2023), fenoprofen (Ogawa et al., 2017), ibuprofen (Braga et al., 2003), ketoprofen (Betlejewska-Kielak et al., 2021), sertraline (Aree, 2021), piroxicam (Chiesi-villa et al., 1998), and aromatic tricyclic drugs (cyclobenzaprine, or amitriptyline) (Castiglione et al., 2017). In addition, there is a few

Table 1
Elemental composition data from SEM analysis of **Na-β-CD** (**A**) and **NaCl-βCD** (**B**).

Sample	Na-βCD			NaCl-βCD			
Element	**C**	**O**	**Na**	**C**	**O**	**Na**	**Cl**
Mass (%)	47.62	50.59	1.79	49.00	45.23	2.50	3.27
Atom (%)	55.03	43.89	1.08	52.74	36.54	1.41	1.19

number of single-crystal X-ray structures of β-CD with other compounds such as benzamide (Wang et al., 2007), succinic, squaric or benzoic acids (Wang et al., 2007; Lisnyak et al., 2007; Crisma et al., 2001), and menthyl-O-D-glucopyranoside (Raffaini et al., 2009). Crystallographic evidences of β-CD ICs were also reported for two organic solvents, namely dimethylsulphoxide (Aree & Chaichit, 2002) and ethanol (Aree & Chaichit, 2003). However, β-CD suffers from limited water solubility (18 mg/L at 25 °C) due to the hydrogen bonds formed between the C2-OH and C3-OH groups of its seven glucopyranose units (Sarabia-Vallejo et al., 2023). Despite the significant potential for the selective modification of β-CD hydroxyl groups *via* processes such as alkylation, oxidation, or doping with cationic metals ions (Řezanka, 2018), its wider application in the formation of β-CD ICs in water remains limitedly explored, with the exception of 2,3,6-trimethyl-β-cyclodextrin with ibuprofen (Brown et al., 1996) and porphyrins (Tsuchiya et al., 2012).

After the serendipitous discovery by the Stoddart's group in 2010 of a new class of porous crystalline alkali metal-cyclodextrin coordination polymers with an extended body-centered three-dimensional open-framework structure, so-called cyclodextrin metal-organic frameworks (CD-MOFs), a renaissance of the research on the IC chemistry of CD-MOFs has been witnessed during the last decade (Smaldone et al., 2010). In fact, CD-MOFs have many potential applications in diverse areas such as templating synthesis of metal-based nanoparticles and gels, guest adsorption and separation, trapping highly reactive intermediates, catalyst supports, sensing, electrical memory, and drug delivery, among others (Roy & Stoddart, 2021).

The first CD-MOFs of empirical formula $[(KOH)_2(C_{48}H_{80}O_{40})\cdot 8H_2O\cdot 8CH_3OH]_n$ and $[(RbOH)_2(C_{48}H_{80}O_{40})\cdot 11H_2O\cdot 2CH_3OH]_n$ were obtained from the reaction of γ-CD and KOH or RbOH after methanol vapor diffusion in aqueous solutions (Smaldone et al., 2010). To our knowledge, the examples of alkali metal-based CD-MOFs with the related β-CD derivative are relatively rare (Sha et al., 2015; Lu et al., 2015; Zhao et al., 2022; Hajra et al., 2021; Liu et al., 2019; Jia et al., 2023; Hu et al., 2021; Rajamohan et al., 2023; Zhao et al., 2024; Zhang et al., 2023; Liu et al., 2017). Until 2015, they were limited to those synthesized using KOH and NaOH (Sha et al., 2015). Subsequently, several studies have reported the synthesis of sodium-based CD-MOFs using β-CD in combination with alternative sodium sources such as $Na_2C_2O_4$ (Lu et al., 2015), Na_2CO_3 (Zhao et al., 2022), and $NaHCO_3$ (Hajra et al., 2021). Similarly, a broader range of potassium sources, including $C_7H_5KO_2$ (Liu et al., 2019), KCl (Jia et al., 2023), KNO_3 (Hu et al., 2021), KH_2PO_4 (Rajamohan et al., 2023), and KI (Zhao et al., 2024; Zhang et al., 2023), has been explored instead of KOH for the formation of potassium-based CD-MOFs. Notably, research on cesium-based CD-MOFs remains particularly scarce, with CsCl being the most commonly used source of alkali metal cations (Liu et al., 2017).

Herein, we report on the preparation of the sodium-based CD-MOF of empirical formula $[Na(C_{42}H_{69}O_{35})\cdot 5H_2O]_n$, abbreviated as **Na-β-CD**, using β-CD and sodium hydride (NaH) as a new source of sodium ions, instead of other sodium sources such as sodium hydroxide (NaOH), sodium oxalate ($Na_2C_2O_4$), and sodium carbonate (Na_2CO_3) or bicarbonate ($NaHCO_3$) (Sha et al., 2015; Lu et al., 2015; Zhao et al., 2022; Hajra et al., 2021). Sodium was selected for its various advantages, including high electronegativity, basic properties, and availability. Using the stronger base NaH is expected to result in the conversion of covalent O–H bonds into ionic Na–O bonds between oxygen from the deprotonated alcohol residues of the glucopyranose units of β-CD and Na^+ ions. Chloride anions were subsequently generated from sodium chloride (NaCl) and incorporated as guest species, leading to the formation of single crystals of the resulting IC of empirical formula $[NaCl(C_{42}H_{70}O_{35})\cdot 9H_2O]_n$, abbreviated as **NaCl-β-CD. Na-β-CD** and **NaCl-β-CD** were characterized using various physico-chemical techniques and spectroscopic methods. Furthermore, **NaCl-β-CD** was subjected to an in-depth structural investigation through single-crystal

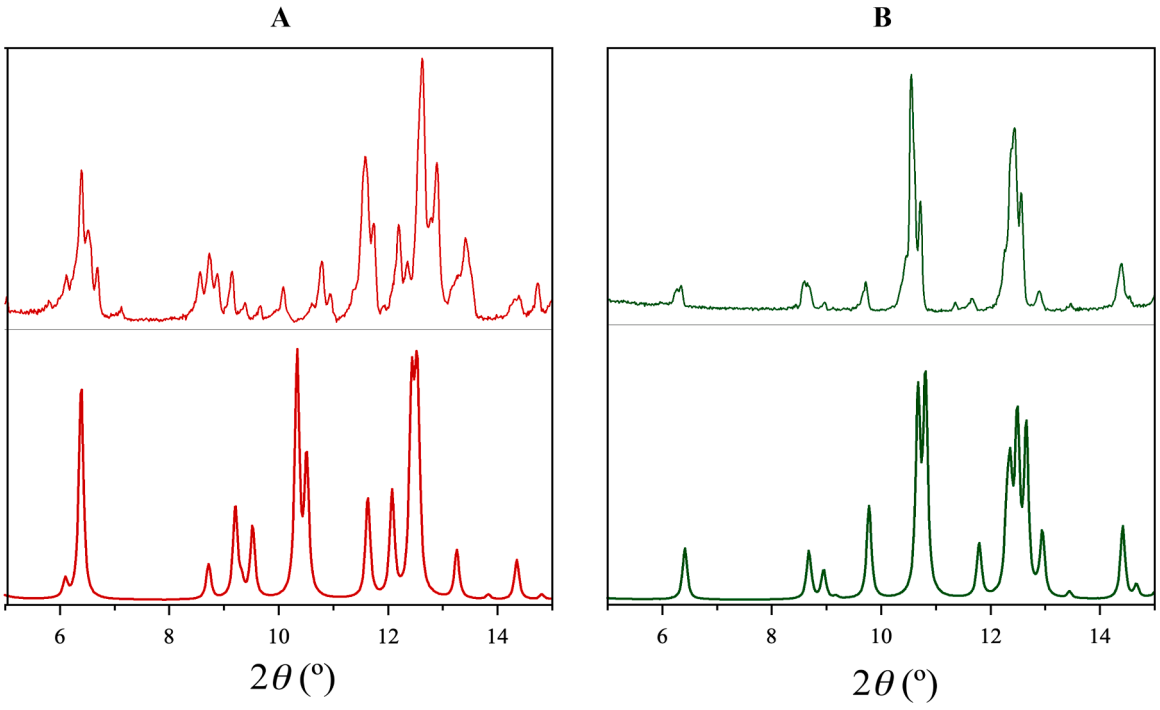

Fig. 3. Experimental XRPD patterns of **Na-β-CD** (**A**) and **NaCl-β-CD** (**B**). The simulated XRPD patterns for **NaOH-β-CD** (**A**) and **NaCl-β-CD** (**B**) are shown as bold lines.

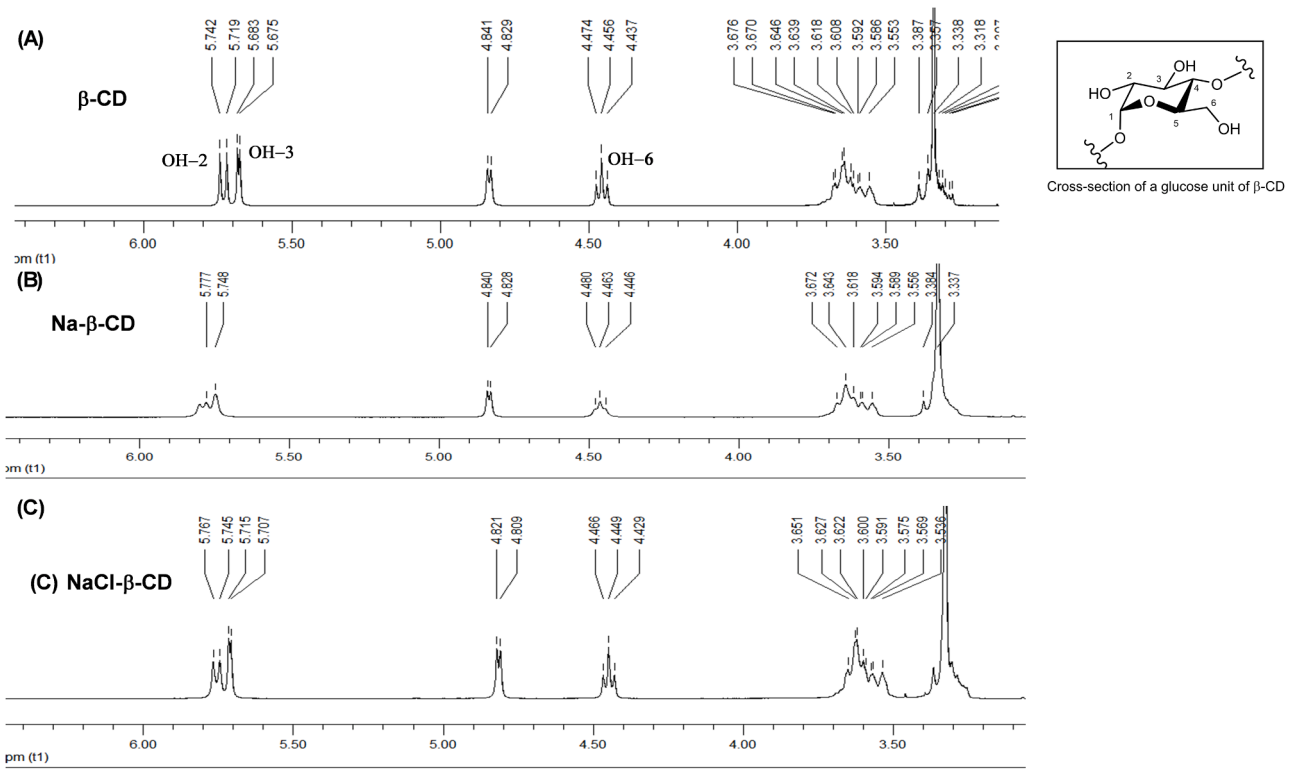

Fig. 4. ^{1}H NMR spectra of β-CD (**A**), **Na-β-CD** (**B**), and **NaCl-β-CD** (**C**). The boxed structure shows the atom numbering scheme of the glucopyranoside unit.

X-ray diffraction (XRD) analysis. Therefore, this work focuses on the use of a new sodium-based CD-MOF (**Na-β-CD**) as a host for the generation of an IC with chloride guest anions (**NaCl-β-CD**) in water/ethanol as solvent medium.

2. Experimental section

2.1. Chemical reagents

Beta-cyclodextrin pentahydrate (β-CD, ≥ 98 %, MW = 1225 g mol^{-1}) was provided from AppliChem, while sodium chloride (NaCl, ≥ 98 %%, MW = 58.44 g mol^{-1}) and dry sodium hydride (NaH, 90 %, MW = 24 g mol^{-1}) were supplied from Sigma Aldrich. On the other side, the dimethylformamide (DMF), tetrahydrofuran (THF), ethanol, and diethyl ether solvents were used in analytical grade, as they were received, without any further purification.

2.2. Physical techniques

Elemental analyses (C, H) were performed at the Servicio Central de Soporte a la Investigación (SCSIE, Valencia, Spain). The SEM-EDX analysis were conducted using scanning electron microscope coupled with an energy-dispersive spectrometer (JEOL, JSM-IT100, Tokyo, Japan) operating at 15 kV. The XRPD data were obtained on a powder X-ray diffractometer (model Ultima IV, Rigaku, Japan) using Cu K_α radiation (λ = 1.5418 Å). FTIR spectra were recorded in the 4000–400 cm^{-1} range with a resolution of 4 cm^{-1} using a Bruker ALPHA II spectrometer equipped with an ATR module. ^{1}H NMR spectra were recorded at room temperature on a Bruker AC 300 spectrometer (300 MHz for proton) using deuterated DMSO-d_6 as solvent.

2.3. Synthesis of Na-β-CD

The preparation of the pentahydrate sodium salt of the monodeprotonated beta-cyclodextrin (**Na-β-CD**) was carried out using the original vapor diffusion method with slight modifications (Xu et al., 2023). Briefly, β-CD (2.15 g, 1.76 mmol) was dispersed in DMF (10 mL), followed by the progressive addition of NaH (0.10 g, 1.76 mmol). The mixture was stirred at room temperature for 2 h, then filtered and transferred to a glass jar containing THF (20 mL) at 4 °C for 14 days. The resulting precipitate was collected by filtration, washed with anhydrous ether, and air-dried, yielding **Na-β-CD**. Yield: 78 %. Elemental analysis calculated for $C_{42}H_{69}NaO_{35}{\cdot}5H_2O$ (MW = 1247 g mol^{-1}): C, 40.45; H, 6.39 %. Found: C, 40.00; H, 6.39 %. FTIR (KBr, cm^{-1}): 3310 (O–H stretching from β-CD and water), 2927 (C–H stretching from β-CD), 1650 and 1595 (H–O–H bending from water). ^{1}H NMR (DMSO-d_6, 300 MHz) δ (ppm): 4.83 (d, H-1), 3.33–3.38 (m, H-2 and H-4), 3.55–3.67 (m, H-3, H-5, and H-6), 5.78 (d, OH-2), 5.748 (s, OH-3), 4.463 (t, OH-6).

2.4. Synthesis of inclusion complex NaCl-β-CD

The preparation of the nonahydrate chloride inclusion complex of the sodium salt of beta-cyclodextrin (**NaCl-β-CD**) was carried out as follows. **Na-β-CD** (0.1 g, 0.08 mmol) was dissolved in 10 mL of an aqueous solution containing NaCl (6.7 mg, 0.08 mmol). The mixture was stirred for 30 min at 60 °C, followed by the dropwise addition of 2 mL of ethanol. The resulting solution was maintained at room temperature for 15 days, leading to the formation of colourless tiny needles of **NaCl-β-CD.** Yield: 88 %. Elemental analysis calculated for $C_{42}H_{70}ClNaO_{35}{\cdot}9H_2O$ (MW = 1356 g mol^{-1}): C, 37.21; H, 6.54 %. Found: C, 37.58; H, 6.59 %. FTIR (KBr, cm^{-1}): 3313 (O–H stretching from β-CD and water), 2920 (C–H stretching from β-CD), 1641 (H–O–H bending from water). ^{1}H NMR (DMSO-d_6, 300 MHz) δ (ppm): 4.82 (d, H-1), 3.31–3.37 (m, H-2 and H-4), 3.53–3.65 (m, H-3, H-5, and H-6), 5.76 (d, OH-2), 5.71 (d, OH-3), 4.45 (t, OH-6).

2.5. Single-crystal X-ray diffraction analysis

X-ray diffraction data on single crystals of **NaCl-β-CD** were collected by means of a Bruker D8 Venture diffractometer with PHOTON II

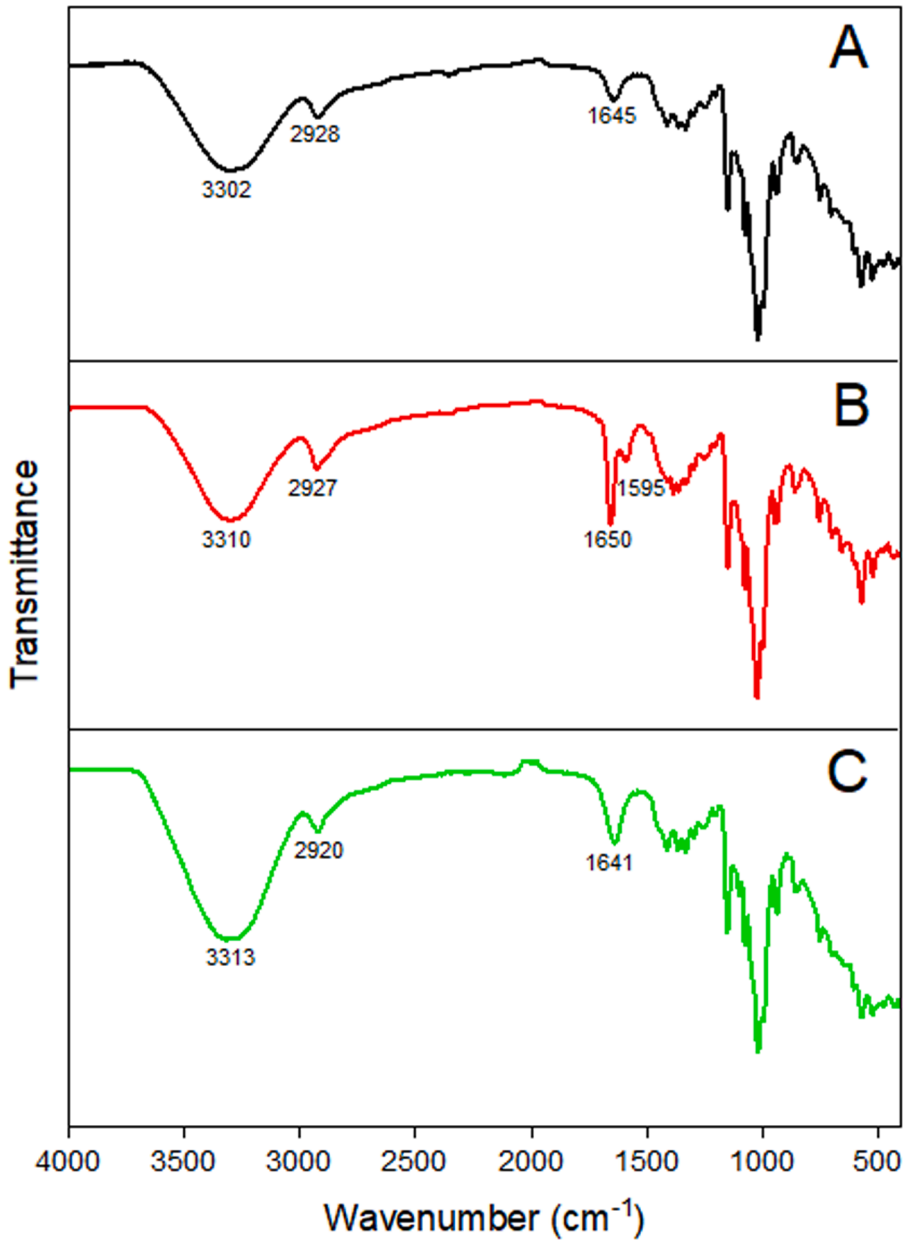

Fig. 5. FTIR spectra of β-CD (**A**), **Na-β-CD** (**B**), and **NaCl-β-CD** (**C**).

detector using monochromatized Mo-K_α radiation ($\lambda = 0.71073$ Å). The structure was solved by standard direct methods and subsequently completed by Fourier recycling by using the SHELXTL software packages. The obtained models were refined with the 2019/3 version of SHELXL against F2 on all data by full-matrix least squares (SHELXTL-2013/4, 2013). **NaCl-β-CD** contains disordered chloride anions and crystallisation water molecules. Three different sites have been identified for both the chloride atom and the associated water oxygen atom, which have been refined with 0.75 (Cl1A and O2Aw), 0.15 (Cl1B and O2Bw), and 0.1 (Cl1C and O2Cw) occupancy factors, while two different sites have been found for another oxygen water atom with 0.75 (O4Aw) and 0.25 (O4Bw). All non-hydrogen atoms were refined anisotropically. The hydrogen atoms from the β-CD molecule were located on a ΔF map and refined isotropically with restraints. Instead, those from the coordinated and crystallization waters were neither found nor calculated. The final calculations were performed with SHELXL, while graphical manipulations were performed with the Crystal Maker program (CrystalMaker, 2015).

Crystallographic data (excluding structure factors) for the structure reported in this paper have been deposited with the Cambridge Crystallographic Data Centre as supplementary publication number CCDC–2474803. Copies of the data can be obtained free of charge by application to CCDC, 12 Union Road, Cambridge CB21EZ, UK (fax: (+44) 1223−336−033; e-mail: deposit@ccdc.cam.ac.uk).

3. Results and discussion

3.1. Physicochemical characterization of Na-β-CD and NaCl-β-CD

3.1.1. SEM and EDX spectra

The morphology and surface of bulk samples of **Na-β-CD** and **NaCl-β-CD** were analyzed by scanning electron microscopy (SEM) at 15.0 kV and 1000 of magnification, as illustrated in Fig. 1. **Na-β-CD** shows agglomerated platelet-like particles and tiny needle-like structures (Fig. 1A). The morphology reveals distinct structural features, deviating from the well-ordered, elongated micro-block morphology typically

Table 2
Summary of crystallographic data for **NaCl-β-CD**.

Formula	$C_{42}H_{88}NaO_{44}Cl$
M (g mol^{-1})	1355.6
Crystal system	Monoclinic
Space group	$P2_1$
a (Å)	15.020(2)
b (Å)	10.1610(13)
c (Å)	20.754(3)
α (°)	90
β (°)	107.983(5)
γ (°)	90
V (Å^3)	3012.7(7)
Z	2
ρ_{calc} (g cm^{-3})	1.474
μ (mm^{-1})	0.183
T (K)	120(2)
Reflect. collcd.	10,666
Reflect. obs. [$I > 2\sigma(I)$]	9414
Data/Restraints/Parameters	10,666/45/829
R_1[a] [$I > 2\sigma(I)$]	0.0586
wR_2[b] [$I > 2\sigma(I)$]	0.1642
S[c]	1.050

[a] $R_1 = \sum(|F_o| - |F_c|)/\sum|F_o|$.
[b] $wR_2 = [\sum w(F_o^2 - F_c^2)^2/\sum w(F_o^2)^2]^{1/2}$.
[c] $S = [\sum w(|F_o| - |F_c|)^2/(N_o - N_p)]^{1/2}$.

reported for other sodium-based β-CD-MOFs (Zhao et al., 2022). In contrast, **NaCl-β-CD** (Fig. 1**B**) exhibits a more compact and irregular morphology, characterized by large, block-like particles with fractured and rough surfaces. Consequently, additional analytical techniques are required to gain deep understanding of the structural features of **Na-β-CD** and **NaCl-β-CD**.

The energy-dispersive X-ray (EDX) spectra of **Na-β-CD** and **NaCl-β-CD** are shown in Fig. 2 and the resulting elemental composition of the samples are summarized in Table 1. The EDX spectra revealed characteristic Na peaks around 1.0 keV for both **Na-β-CD** and **NaCl-β-CD**, while the corresponding Cl peaks around 2.6 keV were exclusively observed for **NaCl-β-CD** (Figs. 2**A** and 2**B**, respectively), confirming the presence of sodium within the **Na-β-CD** structure and both sodium and chloride for **NaCl-β-CD**. Overall, the atomic percentages of C, O, and Na agree with a 1:1 Na/β-CD molar ratio for **Na-β-CD**, while those of C, O, Na, and Cl supports a 1:1:1 Na/Cl/β-CD molar ratio for **NaCl-β-CD.**

3.1.2. XRPD analysis

The XRPD patterns of **Na-β-CD** and **NaCl-β-CD** are compared with the simulated ones for **NaOH-β-CD** and **NaCl-β-CD** in Fig. 3. **Na-β-CD** exhibited prominent diffraction peaks at 6.4, 11.6 and 12.6° (2θ), confirming its crystalline nature (Fig. 3**A**). The different XRPD pattern compared to the related sodium-based β-CD-MOFs of empirical formula $[NaOH(C_{42}H_{70}O_{35})\cdot 9H_2O]_n$ (**NaOH-β-CD**) synthesized using NaOH (2θ = 6.4, 10.3 and 12.5°) (Sha et al., 2015) further supports the successful formation of a new sodium-based β-CD-MOF, whereby the β-CD molecule would be deprotonated under the present synthetic reaction conditions (NaH, DMF). On the other hand, the XRPD pattern of **NaCl-β-CD**, with prominent diffraction peaks at 10.5 and 12.4°, is identical to the simulated one based on the single-crystal X-ray diffraction analysis discussed in the following section, confirming thus the purity and homogeneity of the bulk material (Fig. 3**B**).

3.1.3. ^{1}H NMR spectroscopy

The molecular structures in solution of **Na-β-CD** and **NaCl-β-CD** were further studied using proton NMR spectroscopy. ^{1}H NMR spectra were recorded in deuterated DMSO-d_6 and compared to the parent β-CD, as illustrated in Fig. 4. In the spectrum of β-CD, the protons associated with its carbon skeleton exhibited multiplet signals at δ = 3.31–3.38 (H-2 and H-4), and 3.55–3.67 ppm (H-3, H-5, and H-6) and a doublet signal at δ = 4.83 ppm for H-1 (see the boxed structure in Fig. 4). The protons of the hydroxyl groups display a triplet signal at δ = 4.45 ppm for OH-6 and two doublets at δ = 5.68 and 5.73 ppm for OH-3 and OH-3, respectively. These results were consistent with previous ^{1}H NMR spectroscopic studies (Kou et al., 2024; Hu et al., 2021).

Almost no modification in the chemical shifts were observed for the protons H-1, H-2, H-4, H-3, H-5, and H-6 associated with the carbon skeleton of the β-CD molecule in **Na-β-CD** and **NaCl-β-CD**. However, the protons of the hydroxyl groups, namely OH-2, OH-3 and OH-6, were notably affected, exhibiting slight upward shifts (Fig. 4**B** and **C**, respectively). This can be attributed to their coordination to the sodium cations in deuterated DMSO solution, as can be observed in the crystal structure of **NaCl-β-CD** (*vide infra*). Moreover, these peaks are significantly wider, while their intensity decreased in **Na-β-CD** (Fig. 4**C**), likely due to a rapid proton interchange with the water traces of deuterated DMSO, supporting thus the monodeprotonated nature of the β-CD molecule.

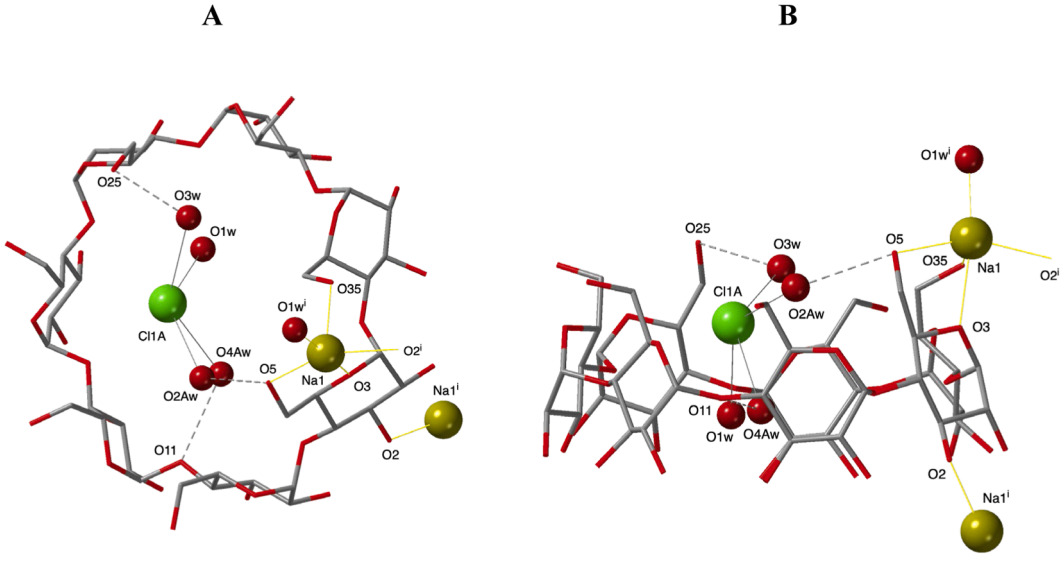

Fig. 6. Top (**A**) and side (**B**) views of the asymmetric unit of **NaCl-β-CD** with the corresponding atom numbering scheme of the sodium and chloride environments [symmetry code: (i) = –x, ½ + y, –z]. The weak coordinative and hydrogen bonding interactions with the sodium and chloride ions are shown as yellow and grey thin lines, respectively, while the hydrogen bonding interactions with the crystallization water molecules are represented by grey dashed lines, respectively (hydrogen atoms are omitted for clarity, as well as the disordered chloride and water oxygen atoms).

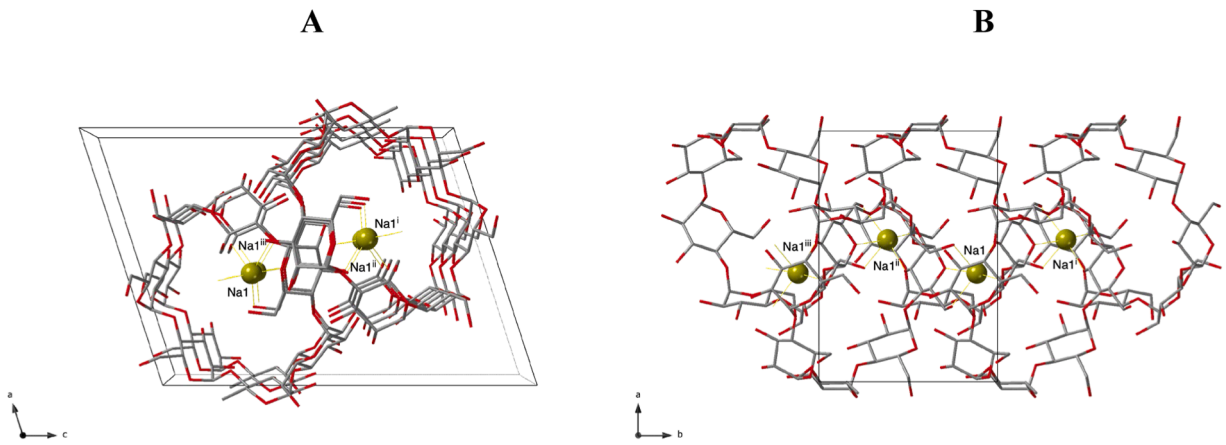

Fig. 7. Top (**A**) and side (**B**) perspective views of a fragment of the double sodium(I)-beta-cyclodextrin chain of **NaCl-β-CD** with the corresponding sodium atom numbering scheme [symmetry code: (i) = –*x*, ½ + *y*, –*z*; (ii) = –*x*, *y* – ½, –*z*; (iii) = *x*, *y* – 1, *z*]. The weak coordinative interactions with the sodium ions are shown as yellow thin lines (hydrogen atoms are omitted for clarity).

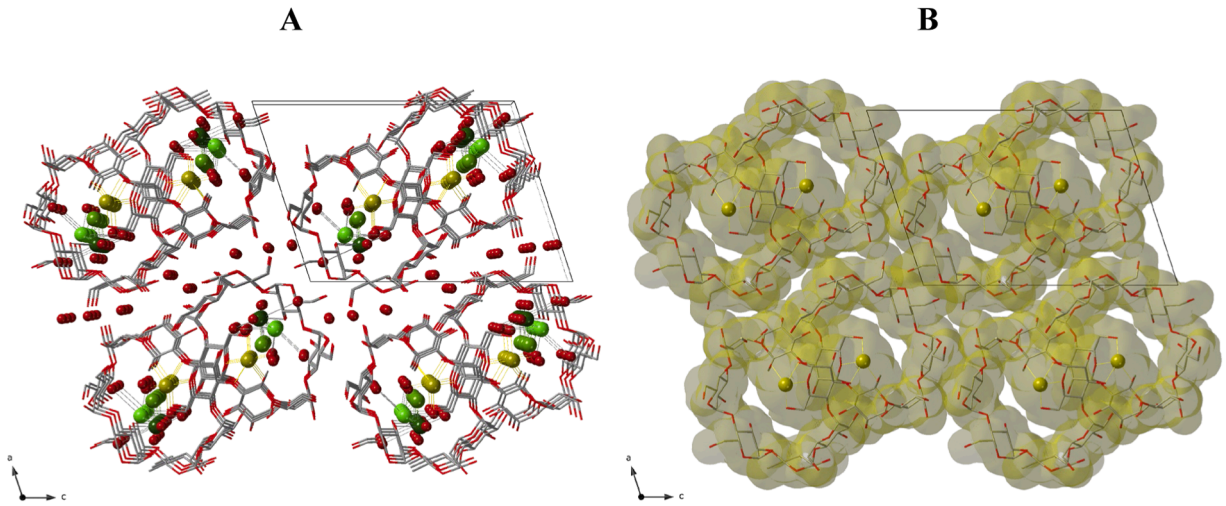

Fig. 8. (A) Perspective view of the crystal packing of **NaCl-β-CD** along the crystallographic *b* axis, showing the filling of the small internal pores and the external interchain space by chloride anions and crystallization waters, respectively. The sodium atoms and crystallization water molecules are represented by yellow and red spheres, while the disordered chloride atoms are shown as green spheres (from light to dark tonalities). (**B**) Surface overlay view of **NaCl-β-CD** without the chloride anions and the water molecules, showing the small internal pores.

3.1.4. FTIR spectroscopy

The chemical groups of β-CD, **Na-β-CD**, and **NaCl-β-CD** were identified *via* Fourier transform infrared (FTIR) spectroscopy, as shown in Fig. 5. The FTIR spectrum of β-CD displayed characteristic peaks at 3302 cm^{-1} for O–H stretching from both the alcohol functions and the crystallization water molecules, 2928 cm^{-1} for symmetric and asymmetric C–H stretching, and a peak at 1645 cm^{-1} corresponding to the H–O–H bending from crystallization water molecules. In general, the FTIR spectra of **Na-βCD** and **NaCl-βCD** are similar to that of β-CD, with only small variations in the intensity of the characteristic peaks for the H–O stretching from crystallization water molecules, as well as the splitting of the peak corresponding to H–O–H bending from crystallization water molecules at 1650 and 1595 cm^{-1}, which is similar to previously reported findings (He et al., 2019; Zhang et al., 2019). This feature could be attributed to weak coordinative or hydrogen bonding interactions of some water molecules with the sodium cations or the chloride anions, respectively, as revealed by the single crystal X-ray diffraction analysis discussed in the following section.

In summary, our findings indicate that **Na-β-CD** and **NaCl-β-CD** exhibit characteristics comparable to those of materials classified as Na-β-CD-MOFs. Elemental and SEM analyses, as well as EDX spectroscopy, are in agreement with the proposed chemical formula for **Na-β-CD** and **NaCl-β-CD** (see Experimental section). Furthermore, FTIR and ^{1}H NMR spectroscopies confirm that the structural framework of beta-cyclodextrin molecule is largely preserved in **Na-β-CD** and **NaCl-β-CD**, with only minor modifications, a trend similarly observed in Na-β-CD-MOFs.

3.2. Description of the structure of NaCl-β-CD

Table 2 summarizes the crystallographic data of **NaCl-β-CD**, while Figs. 6, 7, and 8 illustrate its molecular and crystal structures. It crystallizes in the $P2_1$ space group of the monoclinic system with unit cell dimensions of approximately 15 × 10 × 21 $Å^3$ (Table 2).

In the asymmetric unit, each β-CD molecule with an approximate C_7 molecular symmetry coordinate to one sodium cation and incorporates a chloride ion within its interior cavity (Fig. 6). The Na^+ ion is five-coordinate, bonded to two oxygen atoms from the primary hydroxyl groups (O5 and O35) and one oxygen atom (O3) from the glucose ring of the β-CD molecule, together with one oxygen atom from the secondary hydroxyl group of an adjacent two-fold symmetry-related β-CD molecule ($O2^{i}$) and one additional water molecule ($O1w^{i}$) in an approximate

square pyramidal polyhedron (Na–Ow = 2.29 Å and Na–*O* = 2.32–2.57 Å). On the other hand, the disordered Cl^- ions sitting at the center of the internal cavity of the β-CD molecule are surrounded by oxygen atoms from the coordinated (O1w) and crystallization water molecules (O2Aw, O2Bw, O3w, O4Aw, and O8w), together with one oxygen atom from the secondary hydroxyl group ($O19^i$) of an adjacent two-fold symmetry-related β-CD molecule, *via* weak Cl···H–O hydrogen bonds (Cl···*O* = 3.09 Å and Cl···Ow = 3.11–3.32 Å). Additional weak hydrogen bonding interactions are stablished among some of these water molecules (O2Aw, O3w, and O4Aw) and three oxygen atoms from the primary hydroxyl groups (O5 and O25) and one oxygen atom (O11) linking two contiguous glucose rings of the β-CD molecule (Ow···*O* = 2.82–3.02 Å) that further contribute to stabilize the resulting host-guest $(H_2O)_nCl\subset$β-CD inclusion complex. The Na–Na distance through the bridging glucose ring is 8.33 Å, whereas the Na–Cl distance across the bridging water is 7.25 Å.

The outward coordination of the neutral β-CD molecules to the Na^+ cations in **NaCl-β-CD** gives rise to double sodium(I)-beta-cyclodextrin chains with an overall eight-type double channel configuration growing along the crystallographic *b* axis (Fig. 7), as reported earlier for **NaOH-β-CD** (Sha et al., 2015).

In the crystal lattice, the parallelly disposed double chains are densely packed among each other (Fig. 8), the small interchain space being occupied by additional hydrogen-bonded crystallization water molecules. The hydrated Cl^- anions filling the bowl-like internal pores of the β-CD molecules form linear arrays along the crystallographic *b* axis with a Cl–Cl separation of 10.16 Å (Fig. 8**A**). The calculated void space is *ca.* 30 % of the total unit cell volume and it increases up to *ca.* 40 % without the chloride anions and the water molecules (Fig. 8**B**).

4. Conclusion

In summary, **Na-β-CD** was synthesized by reacting β-CD with sodium hydride as an alternative source of alkali ions, instead of the hitherto employed alkali hydroxides, using vapor diffusion of THF into DMF solution. In the absence of single crystals suitable for X-ray diffraction study, the resulting Na-β-CD-MOF, containing for the first time mono-deprotonated beta-cyclodextrin anions linked by sodium(I) cations, was extensively characterized by using a combination of experimental techniques.

This study further demonstrates the capacity of the synthesized Na-β-CD-MOF to encapsulate chloride ions from aqueous solutions within its interior cavity after protonation of the beta-cyclodextrin molecule from **Na-β-CD** in the aqueous medium. The resulting inclusion complex **NaCl-β-CD** containing neutral β-cyclodextrin molecules linked by sodium(I) cations possessed the typical double-chain structure with bowl-like pores and eight-type double channel configurations filled by chloride anions, as demonstrated by single-crystal X-ray diffraction analyses.

These results demonstrate the ability of **Na-β-CD** to incorporate chloride ions from aqueous solutions, which certainly will pave the way for further research into the selective incorporation of various halide ions such as fluoride anion, expanding the scope of Na-β-CD-MOF materials for the adsorption/removal of halogenated organic compounds from water.

Ethical approval

Not applicable.

Data and code availability

The data supporting the findings of this study are provided within the published article and its supplementary materials available online.

CRediT authorship contribution statement

Amine Ez-zoubi: Writing – review & editing, Writing – original draft, Investigation, Formal analysis, Data curation. **Saskia Merz-Chulbi:** Formal analysis. **Nicolás Moliner:** Software, Formal analysis, Data curation. **Rafael Ruiz-García:** Writing – review & editing, Writing – original draft, Methodology, Formal analysis, Conceptualization. **Abdellah Farah:** Writing – review & editing, Visualization, Formal analysis. **Salah-Eddine Stiriba:** Writing – review & editing, Writing – original draft, Supervision, Project administration, Funding acquisition, Conceptualization.

Declaration of competing interest

The authors declare no competing financial or personal interests influencing this work.

Acknowledgments

We extend our gratitude to the technical staff of the Instituto de Ciencia Molecular (ICMol) for their valuable collaboration in the analysis. We deeply acknowledge Dr. Alexander S. Filatov (University of Chicago) for his assistance with the structural refinement.

Supplementary materials

Supplementary material associated with this article can be found, in the online version, at doi:10.1016/j.carpta.2025.100996.

Data availability

Data will be made available on request.

References

Wang, S., Wei, Y., Wang, Y., & Cheng, Y. (2023). Cyclodextrin regulated natural polysaccharide hydrogels for biomedical applications-a review. *Carbohydrate Polymers, 313*, Article 120760.

Cova, T. F., Murtinho, D., Pais, A. A., & Valente, A. J. (2018). Combining cellulose and cyclodextrins: Fascinating designs for materials and pharmaceutics. *Frontiers in Chemistry, 6*, 271.

Singh, P., & Mahar, R. (2024). Cyclodextrin in drug delivery: Exploring scaffolds, properties, and cutting-edge applications. *International Journal of Pharmaceutics*, Article 124485.

Payamifar, S., & Marjani, A. Poursattar (2024). The recent development of β-cyclodextrin-based catalysts system in click reactions: A review. *Applied Organom Chemis, 38*, e7365.

Payamifar, S., Abdouss, M., & Marjani, A. Poursattar (2024). The recent development of β-cyclodextrin-based catalysts system in Suzuki coupling reactions. *Applied Organom Chemis, 38*, e7458.

Urooj, T., Mishra, M., & Pandey, S. (2024). Unlocking environmental solutions: A review of cyclodextrins in pollutant removal. *Discover Environment, 2*, 65.

Ez-zoubi, A., Boutahiri, N., El Fadili, M., Sghyar, R., Mujwar, S., Moustaid, W., El-Mrabet, A., & Farah, A. (2025). Beta-cyclodextrin inclusion complexes with phenolic synthetic antioxidants: Synthesis, spectroscopic characterisation, molecular modeling, and activity efficiency. *ChemistrySelect, 10*, Article e202405310.

Douhal, A. (2004). Ultrafast guest dynamics in cyclodextrin nanocavities. *Chemical Reviews, 104*, 1955–1976. https://doi.org/10.1021/cr020669j

Crini, G., Fourmentin, S., Fenyvesi, É., Torri, G., Fourmentin, M., & Morin-Crini, N. (2018). Cyclodextrins, from molecules to applications. *Environmental Chemistry Letters, 16*, 1361–1375.

Crini, G. (2014). Review: A history of cyclodextrins. *Chemical Reviews, 114*, 10940–10975.

Kfoury, M., & Fourmentin, S. (2023). Cyclodextrins as building blocks for new materials. *Beilstein Journal of Organic Chemistry, 19*, 889–891. https://www.beilstein-journals.org/bjoc/articles/19/66 (accessed November 18, 2024).

Ez-zoubi, A., Zaroual, H., Zoubi, Y. E., Fadil, M., & Farah, A. (2024). Inclusion complex essential oil into cyclodextrins and its optimization via experimental designs: A review. *Chem. Pap.*

Liu, Z., & Liu, Y. (2022). Multicharged cyclodextrin supramolecular assemblies. *Chemical Society Reviews, 51*, 4786–4827.

Prochowicz, D., Kornowicz, A., & Lewiński, J. (2017). Interactions of native cyclodextrins with metal ions and inorganic nanoparticles: Fertile landscape for chemistry and materials science. *Chemical Reviews, 117*, 13461–13501.

Christoforides, E., Papaioannou, A., & Bethanis, K. (2018). Crystal structure of the inclusion complex of cholesterol in β-cyclodextrin and molecular dynamics studies. *Beilstein Journal of Organic Chemistry, 14*, 838–848.
Aree, T., & Jongrungruangchok, S. (2016). Crystallographic evidence for β-cyclodextrin inclusion complexation facilitating the improvement of antioxidant activity of tea (+)-catechin and (-)-epicatechin. *Carbohydrate Polymers, 140*, 362–373.
Aree, T. (2019). Inclusion complex of β-cyclodextrin with coffee chlorogenic acid: New insights from a combined crystallographic and theoretical study. *Acta Crystallographica Section C: Structural Chemistry, 75*, 15–21.
Nishioka, F., Nakanishi, I., Fujiwara, T., & Tomita, K. (1984). The crystal and molecular structure of the β-cyclodextrin inclusion complex with aspirin and salicylic acid. *Journal of Inclusion Phenomena, 2*, 701–714.
Borodi, G., Bratu, I., Dragan, F., Peschar, R., Helmholdt, R. B., & Hernanz, A. (2008). Spectroscopic investigations and crystal structure from synchrotron powder data of the inclusion complex of β-cyclodextrin with atenolol. *Spectrochimica Acta Part A: Molecular and Biomolecular Spectroscopy, 70*, 1041–1048.
Betlejewska-Kielak, K., Bednarek, E., Budzianowski, A., Michalska, K., & Maurin, J. K. (2023). Comprehensive characterisation of the flurbiprofen/β-cyclodextrin inclusion complex using X-ray techniques and NMR spectroscopy. *Journal of Molecular Structure, 1285*, Article 135450.
Ogawa, N., Nagase, H., Loftsson, T., Endo, T., Takahashi, C., Kawashima, Y., Ueda, H., & Yamamoto, H. (2017). Crystallographic and theoretical studies of an inclusion complex of β-cyclodextrin with fentanyl. *International Journal of Pharmaceutics, 531*, 588–594.
Braga, S. S., Gonçalves, I. S., Herdtweck, E., & Teixeira-Dias, J. J. (2003). Solid state inclusion compound of S-ibuprofen in β-cyclodextrin: Structure and characterisation. *New Journal of Chemistry, 27*, 597–601.
Betlejewska-Kielak, K., Bednarek, E., Budzianowski, A., Michalska, K., & Maurin, J. K. (2021). Comprehensive characterisation of the ketoprofen-β-cyclodextrin inclusion complex using x-ray techniques and nmr spectroscopy. *Molecules, 26*, 4089.
Aree, T. (2021). Advancing insights on β-cyclodextrin inclusion complexes with SSRIs through lens of X-ray diffraction and DFT calculation. *International Journal of Pharmaceutics, 609*, Article 121113.
Chiesi-villa, A., Rizzoli, C., Amari, G., Delcanale, M., Redenti, E., & Ventura, P. (1998). The crystal structure of the inclusion complex of the Sodium salt of Piroxicam with β-cyclodextrin. *Supramolecular Chemistry, 10*, 111–119.
Castiglione, F., Ganazzoli, F., Malpezzi, L., Mele, A., Panzeri, W., & Raffaini, G. (2017). Inclusion complexes of β-cyclodextrin with tricyclic drugs: An X-ray diffraction, NMR and molecular dynamics study. *Beilstein Journal of Organic Chemistry, 13*, 714–719.
Wang, E.-J., Lian, Z.-X., & Cai, J. (2007). The crystal structure of the 1: 1 inclusion complex of β-cyclodextrin with benzamide. *Carbohydrate Research, 342*, 767–771.
Lisnyak, Y. V., Martynov, A. V., Baumer, V. N., Shishkin, O. V., & Gubskaya, A. V. (2007). Crystal and molecular structure of β-cyclodextrin inclusion complex with succinic acid. *Journal of Inclusion Phenomena and Macrocyclic Chemistry, 58*, 367–375.
Crisma, M., Fornasier, R., & Marcuzzi, F. (2001). The crystal structure of the 1: 1 inclusion complex of β-cyclodextrin with squaric acid. *Carbohydrate Research, 333*, 145–151.
Raffaini, G., Ganazzoli, F., Malpezzi, L., Fuganti, C., Fronza, G., Panzeri, W., & Mele, A. (2009). Validating a strategy for molecular dynamics simulations of cyclodextrin inclusion complexes through single-crystal X-ray and NMR experimental data: A case study. *Journal Physics Chemistry B, 113*, 9110–9122.
Aree, T., & Chaichit, N. (2002). Crystal structure of β-cyclodextrin–dimethylsulfoxide inclusion complex. *Carbohydrate Research, 337*, 2487–2494.
Aree, T., & Chaichit, N. (2003). A new crystal form of β-cyclodextrin–ethanol inclusion complex: Channel-type structure without long guest molecules. *Carbohydrate Research, 338*, 1581–1589.
Sarabia-Vallejo, Á., Caja, M.del M., Olives, A. I., Martín, M. A., & Menéndez, J. C. (2023). Cyclodextrin inclusion complexes for improved drug bioavailability and activity: Synthetic and analytical aspects. *Pharmaceutics, 15*, 2345.
Řezanka, M. (2018). Synthesis of cyclodextrin derivatives. In S. Fourmentin, G. Crini, & E. Lichtfouse (Eds.), *Cyclodextrin fundamentals, reactivity and analysis* (pp. 57–103). Cham: Springer International Publishing.
Brown, G. R., Caira, M. R., Nassimbeni, L. R., & Oudtshoorn, B. (1996). Inclusion of ibuprofen by heptakis(2,3,6-tri-O-methyl)-?-cyclodextrin: An X-ray diffraction and thermal analysis study. *Journal of Inclusion Phenomena and Macrocyclic Chemistry, 26*, 281–294.
Tsuchiya, Y., Shiraki, T., Matsumoto, T., Sugikawa, K., Sada, K., Yamano, A., & Shinkai, S. (2012). Supramolecular dye inclusion single crystals created from 2,3,6-trimethyl-β-cyclodextrin and porphyrins. *Chemistry A European J, 18*, 456–465.
Smaldone, R. A., Forgan, R. S., Furukawa, H., Gassensmith, J. J., Slawin, A. M., Yaghi, O. M., & Stoddart, J. F. (2010). Metal-organic frameworks from edible natural products. *Angew Chem Int Ed, 49*, 8630–8634.
Roy, I., & Stoddart, J. F. (2021). Cyclodextrin metal–Organic frameworks and their applications. *Accounts of Chemical Research, 54*, 1440–1453.
Sha, J.-Q., Wu, L.-H., Li, S.-X., Yang, X.-N., Zhang, Y., Zhang, Q.-N., & Zhu, P.-P. (2015). Synthesis and structure of new carbohydrate metal–organic frameworks and inclusion complexes. *Journal of Molecular Structure, 1101*, 14–20.
Lu, H., Yang, X., Li, S., Zhang, Y., Sha, J., Li, C., & Sun, J. (2015). Study on a new cyclodextrin based metal–organic framework with chiral helices. *Inorganic Chemistry Communications, 61*, 48–52.
Zhao, P., Huang, L., Wang, H., Wang, C., Chen, J., Yang, P., Ni, M., Chen, C., Li, C., & Xie, Y. (2022). An ultrasensitive high-performance baicalin sensor based on C3N4-SWCNTs/reduced graphene oxide/cyclodextrin metal-organic framework nanocomposite. *Sensors and Actuators B: Chemical, 350*, Article 130853.
Hajra, S., Sahu, M., Padhan, A. M., Lee, I. S., Yi, D. K., Alagarsamy, P., Nanda, S. S., & Kim, H. J. (2021). A green metal–Organic framework-cyclodextrin MOF: A novel multifunctional material based triboelectric nanogenerator for highly efficient mechanical energy harvesting. *Adv Funct Materials, 31*, Article 2101829.
Liu, C., Wang, P., Liu, X., Yi, X., Zhou, Z., & Liu, D. (2019). Multifunctional β-cyclodextrin MOF-derived porous carbon as efficient herbicides adsorbent and potassium fertilizer. *ACS Sustainable Chem. Eng., 7*, 14479–14489.
Jia, J., Liu, Y., Wu, D., Yu, J., Gao, T., & Li, F. (2023). Water-insoluble β-cyclodextrin-based nanocubes as cost-effective adsorbents for dyeing wastewater remediation with high selectivity. *Chemical Engineering Journal, 457*, Article 141331.
Hu, Z., Li, S., Wang, S., Zhang, B., & Huang, Q. (2021a). Encapsulation of menthol into cyclodextrin metal-organic frameworks: Preparation, structure characterization and evaluation of complexing capacity. *Food Chemistry, 338*, Article 127839.
Rajamohan, R., Ashokkumar, S., Murali Krishnan, M., Murugavel, K., Murugan, M., & Lee, Y. R. (2023). Adenosine/β-cyclodextrin-based metal–Organic frameworks as a potential material for cancer therapy. *Biomolecules, 13*, 1154.
Zhao, X., Li, T., Guo, T., He, X., Ren, X., Wang, M., Wang, C., Peng, C., Zhang, J., & Wu, L. (2024). Supramolecular structure of the β-cyclodextrin metal–Organic framework optimizes iodine stability and its Co-delivery with L -Menthol for antibacterial applications. *ACS Appl. Mater. Interfaces, 16*, 24235–24247.
Zhang, Y., Chen, J., Zhang, Z., Zhu, H., Ma, W., Zhao, X., Wang, M., Wang, C., Chen, W., Naeem, A., Zhang, J., Guo, T., & Wu, L. (2023). Solvent-free loading of vitamin A palmitate into β-cyclodextrin metal-organic frameworks for stability enhancement. *AAPS PharmSciTech, 24*, 136.
Liu, J., Bao, T.-Y., Yang, X.-Y., Zhu, P.-P., Wu, L.-H., Sha, J.-Q., Zhang, L., Dong, L.-Z., Cao, X.-L., & Lan, Y.-Q. (2017). Controllable porosity conversion of metal-organic frameworks composed of natural ingredients for drug delivery. *Chemical Communications, 53*, 7804–7807.
Xu, Y., Rashwan, A. K., Osman, A. I., Abd El-Monaem, E. M., Elgarahy, A. M., Eltaweil, A. S., Omar, M., Li, Y., Mehanni, A.-H. E., Chen, W., & Rooney, D. W. (2023). Synthesis and potential applications of cyclodextrin-based metal–organic frameworks: A review. *Environmental Chemistry Letters, 21*, 447–477.
SHELXTL-2013/4. (2013). *Bruker analytical X-ray instruments*. Madison, WI, USA: Bruker. n.d.
CrystalMaker. (2015). *CrystalMaker software*. England: Bicester. n.d.
Kou, X., Xu, X., Gao, N., Zhang, Y., Huang, X., Chen, F., Ke, Q., & Meng, Q. (2024). Supramolecular chemistry in cyclodextrin inclusion complexes: The formation rules of terpenes/β-cyclodextrin inclusion complexes. *Food Hydrocolloids, 157*, Article 110441.
Hu, Y., Qiu, C., McClements, D. J., Qin, Y., Fan, L., Xu, X., Wang, J., & Jin, Z. (2021b). Simple strategy preparing cyclodextrin carboxylate as a highly effective carrier for bioactive compounds. *Journal of agricultural and food chemistry, 69*, 11006–11014.
He, Y., Zhang, W., Guo, T., Zhang, G., Qin, W., Zhang, L., Wang, C., Zhu, W., Yang, M., & Hu, X. (2019). Drug nanoclusters formed in confined nano-cages of CD-MOF: Dramatic enhancement of solubility and bioavailability of azilsartan. *Acta Pharmaceutica Sinica B, 9*, 97–106.
Zhang, B., Huang, J., Liu, K., Zhou, Z., Jiang, L., Shen, Y., & Zhao, D. (2019). Biocompatible cyclodextrin-based metal–Organic frameworks for long-term sustained release of fragrances. *Ind Eng Chemistry Res, 58*, 19767–19777.